PDC Bits: All comes from the cutter rock interaction

Laurent Gerbaud, Stephane Menand, Hedi Sellami

IADC/SPE 98988

PDC Bits : All Comes From the Cutter Rock Interaction

L.Gerbaud, S.Menand, H.Sellami, Ecole des Mines de Paris

This paper was prepared for presentation at the IADC/SPE Drilling Conference held in Miami, Florida, U.S.A., 21–23 February 2006.

Abstract

PDC drill bit performances in hard rock has been greatly improved during the last decades by innovations in PDC wear, impact resistance and better vibrations understanding. The bit design is generally done by balancing the bit, distributing uniform wear along the profile and achieving high drillability and steerability. To obtain required drilling performances, drill bit designer adjust features such as profile shape, gage and mainly cutter characteristics (shape, type and orientation). Cutter rock interaction model became a critical feature in the design process. But previously used models considered only three forces on a cutter based on the cutter-rock contact area : drag force, normal force and side force. Such models are no longer valid with the introduction of PDC cutters with chamfer and special shape.

This paper presents a new cutter rock interaction model including some several improvements. It is based on the presence of a build-up edge of crushed materials on the cutting face often described in the literature. In addition, the chamfer, which significantly affects bit Rate Of Penetration (ROP), is taken into account (shape and size). Forces applied on the back of the cutter and due to the rock deformation and back flow of crushed materials are considered in the model. Finally, results of numerous single cutter tests (under atmospheric and confining pressure) are presented and compared to the new cutter rock interaction model predictions. An analysis of the influence of the PDC characteristics (shape, size, chamfer, back and side rake angles, ….) is presented.

The model has been applied to optimize the cutting efficiency and bit steerability and some design rules are given to minimize the specific energy and maximize the rate of penetration. Finally, full scale laboratory drilling tests and field results indicate that the use of accurate cutter rock interaction model can help the drill bit designer to find the best drill bit for a specific application. Standard laboratory full scale drilling procedures have been developed. The tests have shown that drillability, stability, steerability and wear can be improved and controlled by acting on the cutter characteristics, cutter setup, trimmer characteristics and gage type.

Introduction

Since their introduction in the 1970's, PDC drill bit performances increase continuously by improving PDC technology[1], cutting structure[2,3], dynamic stability[4,5], hydraulic[6] and steerability[7] to drill more and more smoothly and rapidly. Now, with the development of surface and downhole drilling parameters measurements, real time performance analysis[8] become the key of the future drilling performance improvement. Real time performance analysis allows to optimize the drilling parameters[9] to reach the optimum ROP while post analysis helps the driller to choose the best bit adapted to a specific application.

What is common with the major part of all the previous topics ? The cutter rock interaction process. Indeed, to estimate the bit drillability versus the nature of formations to be drilled, to calculate the imbalance force for stabilization, to determine the bit steerability, we need to know what are the elementary cutter forces and how you can handle them. Furthermore, to optimize the drilling parameters in order to increase the ROP, you need to know the real drill bit response which is a direct function of the cutter rock interaction.

While abondent literature deals with PDC bit design, there is no progress in the cutter rock interaction understanding and modeling since many years. It is generally assumed both in analytical[10,11] and empirical[12] models, that the magnitude of the cutting force acting on a cutter, while cutting a groove in a rock sample, is proportional to the cut surface area. This modeling gives good results with sharp cutter (15° back rake angle) but when you change back rake angle or use chamfered cutters, theoretical results do not fit with experimental results[13] and give higher cutter forces when increase back rake angle compared to experimental results. Although the importance of chamfer and back face cutter have been outlined in some recent papers[1,2], no modelling of these effects on the cutting forces have been done. To improve PDC bit performance and design, it is now very important to take into account this phenomena.

The new cutter rock interaction model presented in this paper consider the effect of side and back rake angle by introducing a build-up edge of crushed materials on the cutting face. The use of crushed materials provided a better force estimation . Chamfer size and shape effects are also modeled as well as rock deformation on the back cutter.

New cutter-rock interaction model has been applied to drill bit design. Full scale laboratory drilling tests and field trials show significant improvements in bit drillability by optimizing cutting efficiency playing on cutter shape and cutter orientation. At the end of this paper, several design concepts and features including energy minimization, balancing and steerability are presented.

Cutter Rock Interaction Model

Consider a cylindrical chamfered PDC cutting a groove on the surface of a rock sample at constant depth of cut. The cutter inclination is defined by the back rake angle ω_c and the side rake angle ω_s. During the cutting process, a force is applied on the rock by the cutter in order to create a chip and to maintain a constant depth of cut (**Figure 1**). Previous models[10,11,12] considered only one force applied on the cutting face. Such a model is no longer valid with the introduction of PDC cutters with a chamfered geometry, which significantly affects bit ROP and WOB/TOB relationship. Furthermore, laboratory tests[13] have found that the orientation of PDC cutter relative to rock surface (back rake and side rake angle) play a significant role in the determination of cutting forces; the previous models highly overestimate the effects of these angles. In the new cutter rock interaction model, the total force acting on the PDC cutter is divided here into three groups (**Figure 2**): forces acting on the cutting face surface denote F^c, forces acting on the chamfer surface denote F^{ch} and forces acting on the back cutter surface denote F^b:

$$F = F^c + F^{ch} + F^b \tag{1}$$

Cutting face force. Generally considered as the pure cutting force, the cutting face force is used for destroying the rock. Previously, it was generally assumed in literature[10,11,12] that the horizontal (in the direction of the cutter velocity) and vertical (normal to the rock surface) forces were proportional to the cross-section area A of the cut :

$$\begin{aligned} F_c^c &= R_{eq} * A \\ F_n^c &= \tan(\theta_f + \omega_c) * R_{eq} * A \end{aligned} \tag{2}$$

Where the constant R_{eq} is defined as the intrinsic specific energy or rock equivalent strength and θ_f is the rock-cutter friction angle at the rock-cutter interface. Laboratory observations show the presence of a build-up edge of crushed materials on the cutting face which controls the flow of failed material. The new cutting force model takes into account this phenomena by introducing this crushed material[14]. As shown on **Figure 3**, the model considers that the force applied by the cutting face is transferred to the rock through the build-up edge of a crushed material. The direct consequence is a constant single chip failure plane independent of PDC orientation and characterized by Ψ angle. Back and side rake angles affect the cutting face force only trough the frictional contact between the build up of crushed material and the rock surface. By considering that cutter width is large compared to the depth of the cut and using a Morh-Coulomb criteria, the cutting face force can be expressed by equations 3 :

$$\begin{aligned} F_c^c &= \sigma_0 * (1 + k * \tan(\phi') * \tan(\omega_c)) * A \\ F_n^c &= \sigma_0 * (\tan(\theta_f) + k * \tan(\omega_c)) * A \end{aligned} \tag{3}$$

where k is the ratio between the horizontal contact surface of the crushed zone and the product A*tan(ωc), σ_0 is the hydrostatic stress in the crushed material and φ' the friction angle between the crushed rock and the virgin rock.
σ_0 is obtained by chip equilibrum (**figure 3**) and defined by :

$$\sigma_0 = \frac{C_0 + P_b * (\sin(\psi) * \cos(\psi) + \cos^2(\psi) * \tan(\varphi)}{(1 - \tan(\theta_f) * \tan(\varphi)) * (\sin(\psi) * \cos(\psi) - \tan(\theta_f + \varphi) * \sin^2(\psi))} \tag{4}$$

where Co is rock cohesion, φ the rock internal friction angle and Pb the mud pressure.
φ' is defined by[15] :

$$\tan(\varphi') = \frac{\pi}{2} * \tan(\varphi) \tag{5}$$

Chamfer force. Present on the PDC cylindrical tip, the chamfer was introduced to avoid diamond chipping when drilling hard formations. Although all PDC cutters are chamfered, the chamfer forces are rarely considered in literature. Two different mechanisms take place at the chamfer with respect to the depth of cut. If the depth of cut is greater than the chamfer height, crushed rock is trapped between the cutting face and the rock and additional forces are generated in the same way than for the cutting face crushed material. As shown on the **figure 4**, the chamfer forces are the results of the additional friction surface on the bottom of the groove and can be expressed by :

$$\begin{aligned} F_c^{ch} &= \sigma_0 * \tan(\varphi') * A_{ch} \\ F_n^{ch} &= \sigma_0 * A_{ch} \end{aligned} \tag{6}$$

where A_{ch} is the chamfer surface area projection on a horizontal plane.

Now, if depth of cut is lower than chamfer height, the chamfer becomes the cutting face with higher back rake angle and the chamfer forces are the cutting face forces. For example, at 45° chamfer angle and 15° back rake angle, the real back rake angle for small depth of cut becomes 60°.

Back cutter forces. In addition to the cutting face forces and the chamfer forces, it has been shown[16] using an elasto plastic rock behaviour model that some deformation appeared on the back of the cutter during the cutting process (**figure 5**) and thus applied additional forces on the cutter. Furthermore, laboratory observations have shown that a part of the crushed material is driven on the back of the cutter. As shown on the **figure 6**, the stresses on the back of the cutter vary linearly from the hydrostatic pressure σ_0 in the crushed rock zone at the tip of the cutter to 0 at the repression end point with an angle α which is assumed to be a rock property.

The back cutter forces can be expressed by :

$$F_c^b = \sigma_0 * f(\alpha, d, \omega_d)$$
$$F_n^b = F_c^b * f_1(\alpha, d, \omega_d) \quad (7)$$

where d is the depth of cut and ω_d the relief angle.

wear forces. When drilling hard and abrasive formations, PDC cutter is wearing and a wear surface parallel to the rock surface appear on the cutter. Additional forces are generated at the wearflat area-rock surface contact. As wearflat appears, back cutter forces and chamfer forces disappear. Wear forces can be expressed by :

$$F_c^f = \sigma_0 * \mu * A_f$$
$$F_n^f = \sigma_0 * A_f \quad (8)$$

where A_f is the wearflat area and μ is the interfacial friction angle between wearflat and rock.

Experimental data

Extensive series of single cutter experiments were carried at the Ecole des Mines de Paris under atmospheric as well as mud pressure conditions. All the cutting tests were performed at constant cutting speed under imposed depth of cut d. Tests were carried out with sharp and chamfered cutters of diameter 8, 13 and 19 mm.

Experimental setup. The tests were conducted on a linear single cutter test-stand (**figure 7**) for atmospheric test and in a drilling cell (**figure 8**) for confinement tests. During each test, the forces are recorded in 3 directions and the operating parameters are controlled.

Experimental procedure. The test procedure consists in making groove at constant depth of cut on the planned surface of the rock sample. The tests were carried out in three steps :

- move up the cutter to tangent the cutting edge with the free surface of the rock sample,
- adjust the depth of cut with respect to the tangency point,
- cut the groove at constant velocity of 25 cm/min and record the cutting forces

Rock materials. Most of the cutting tests were carried out in Vosges Sandstone (compressive strength = 36 MPa, Cohesion = 10 MPa, internal friction angle = 35°) which is an homogeneous and medium strength rock. The cutting process is dominated by ductile failure and brittle failure is negligible. Additional tests were carried out in Buxy limestone which is a harder rock (Compressive strength = 85 MPa).

Experimental program. In order to demonstrate the good relation between experimental data and the new cutter rock interaction model, numerous single cutter tests were done with different experimental setup. Tests have been done in order to assess and analyse separately the different forces listed before. During each test, the three force components were recorded at at a sampling rate of 500 Hz. **Figure 9** shows an example of experimental results where we can observe the cutting process along time. For each force component, an average value of the maximum force is obtained, corresponding to the cutting removal.

For the cutting face force and the presence of the build up edge of crushed rock, tests were carried out with sharp cutter and different back and side rake.

For the chamfer forces, comparison were made between sharp and chamfer cutter under the same conditions (constant orientation, same rock, same experimental device, same test procedure).

Finally, to observe the back cutter forces, tests were carried out at constant back rake angle with different relief angle.

Analysis of experimental results. The assumption regarding the presence of a build up edge of crushed rock between the cutter face and the rock chipping is demonstrated by the laboratory experiments and the numerical simulations. If we consider previous cutter rock interaction models, the normal and tangential forces are overestimated when back rake angle is increased over 20°. The new cutter rock interaction model gives a good relation with experimental results when increasing back rake angle with sharp cutter (**Figure 10**). Indeed, the introduction of a build up edge of crushed rock reduces the impact of the back rake angle. The forces corresponding to the chipping action remain independant from bake rake angle. The additional force is due to the friction between the crushed zone and the groove. With the same assumption, **figure 11** shows the theoretical and experimental evolutions of the normal force as a function of side rake angle at 1.5 mm depth of cut during an assymetric cut (distance to adjacent groove equal to 6 mm). Forces increase with a good accuracy between expriments and theory. The lateral force increases slowly with respect to the side rake increase (**Figure 12**).

Figure 13 shows the normal force evolution versus depth of cut for sharp and chamfered PDC cutters. We can observe that normal chamfer force represent 40% of the total normal forces at 2 mm depth of cut but more than 50 % at smaller depth of cut. Force recording (**Figure 14**) during single cutter tests at very low depth of cut (0.15 mm) shows no difference between sharp cutter with 60° back rake angle and chamfered cutter with 15° back rake angle and 45° chamfered angle. These observations validate the major influence of the chamfer on the total forces and the importance of depth of cut in the chamfer.

During special single cutter tests using pre existing hole before the groove to be cut[17] (no contact between the cutter and the bottom of the groove cut), rock cutter friction angle was estimated to 10°. When considering the normal force versus the tangential force for a sharp cutter (**figure 15**), we obtained an experimental rock cutter friction angle greater and equal to 20°. So, we consider that the additional force is generated at the back cutter face. For a 13 mm PDC diameter with 15° back rake angle and 10° friction angle we obtained an α angle, which is a rock characteristic, equal to 11°. This conclusion was verified using various cutting tests; the back cutter force increase while reducing the relief angle.

PDC Bit Design

Cutter layout of a PDC bit is one of the most important features in PDC bit design. Indeed, cutter layout acts directly on bit drillability, wear of cutters over the bit face, bit stability and bit steerability. The development of the new cutter rock interaction model described in this paper allows significant advancements in all these topics.

ROP improvement. Let consider the drilling strength ζ as the ratio between the normal cutting force and the cross section area :

$$\zeta = \frac{F_n}{A} \quad (9)$$

Theoretical model and results of PDC cutter tests (**figure 16**) show that the drilling strength has a minimum function of distance to adjacent pre-existing cuts[18]. This minimum is also a function of the depth of cut. When applying this concept to the PDC bit, major improvement can be made and optimized PDC bit cutter layout can be chosen with regard to ROP.

Full scale drilling bench tests (**figure 17**) were conducted in order to demonstrate the cutter layout importance in bit drillability. Special PDC bits have been designed for these tests (**Figure 18**). **Figure 19** shows that at low ROP, the high cutters density bit drills faster than the low cutters density bit because lateral distance between PDC needs to be small. At higher ROP, the low cutters density bit drills faster, which is coherent with drilling strength optimization.

Bit Stability. There are two design principles to improve bit stability : anti-whirl PDC bit design and global balanced PDC bit design. Anti-whirl PDC[5] bit design consists in generating a resultant radial force directed toward a specific low friction portion of the bit. The negative effect of this technology is energy loss du to additional friction on the gage pad.

The global balanced PDC bit principle[1] is different. PDC cutters are arranged so that the resultant radial force and bending moments are minimized. Resultant radial force contributes to bit lateral motion and whirl. Bending moments contribute also to bit lateral motion and also to bit tilt motion which have an effect on bit stability and directional control. A PDC bit with both radial force and bending moment balanced is more stable. The new PDC-rock interaction model allows to achieve this goal.

Bit directional control. The bit directional behaviour is controlled by the main following characteristics : the bit sterrability and the walk angle[7]. The bit design for a specific directional application must also take into account the dircetional system used, that plays a major role in the deviation process.

The bit steerability corresponds to the ability of the bit, submitted to lateral and axial forces, to initiate a lateral deviation. Bit steerability is defined[19] by the ratio of the lateral drillability (D_{lat}) over the axial drillability (D_{ax}). PDC bits side cutting capabilities become essential to increase bit steerability. Steerable PDC bits are generally chosen for "push the bit" rotary steerable systems (RSS), although low steerable PDC bits are prefered for "point the bit" RSS. The walk angle is the angle measured in a plane perpendicular to the bit axis, between the direction of the side force applied to the bit and the direction and the direction of the lateral displacement of the bit[7].

Another critical factor in directional system deviation control is the bit tilt. The bit tilt is defined as the angle between the bit axis of rotation and the tangent of the wellpath, and is mainly controlled by the directional system : rotary bottom hole assembly, steerable assembly or RSS. The directional behaviour of the drilling system is then a complex coupling between bit directional responsiveness and mechanical behaviour of the directional system (side force and bit tilt effects), while having in mind a possible rock-formation effect[20] (interbedded or laminated formations).

Whatever the directional system used to deviate the wellbore, one need to estimate the bit steerability and the walk angle of the PDC bits. The cutter rock interaction model is then critical, as it enables to evaluate within the PDC bit performance evaluation software, the bit directional responsiveness in any type of rock formation.

Field Applications

The new cutter rock interaction model described in this paper have provided several improvements in term of drilling performances. For example, in a slim hole project in Gabon[2], a special bit has been designed incorporating these design principles. The newly designed bit drilled successfully 671 m at an average ROP of 11 m/h whereas previous bit drilled the same length at an average ROP of 4.3 m/h. In this case, the PDC bit performance improvement was obtained by the utilisation of the minimum energy concept and better stabilisation. Another application concerned the design and the run of PDC bits having left, rigth or neutral directional tendencies. This application provided a new classification of PDC bits according to their steerability[19].

Conclusions.

Cutter rock interaction is very important in drill bit design due to its great effect on ROP, stability and bit steerability. A new cutter rock interaction model was developped for taking into account the new evolution in PDC technologies and the recent experimental observations.

The build up edge of crushed material modeling provides a good evaluation of back and side rake effect on PDC forces.

The chamfer modeling allows direct estimation of the chamfer shape and size on the PDC forces.

The introduction of the back cutter forces provides a good evaluation of the cutter forces and add more optimization possibilities.

The innovations incoporated into this model and described in this paper provide a number of benefits in terms of ROP improvement, bit stability, bit wear and bit directional control.

Nomenclature

A	=	cross section area of the cut, mm²
Ach	=	chamfer surface area on a horizontal plane, mm²
A_f	=	PDC wear flat area, mm²
d	=	Depth Of Cut, mm
F	=	Total force acting upon PDC, N

F^b = Force acting upon the back cutter face, N
F^c = Force acting upon the cutter face, N
F_c = PDC Cutting force, N
F^{ch} = Force acting upon the cutter chamfer, N
F^f = Force acting upon the PDC wear flat, N
F_l = PDC Lateral force, N
F_n = PDC Normal force, N
k = ratio between the projection of the crushed zone on the surface parallel to the rock surface and cutting area
Req = Rock intrinsic specific energy, MPa
ROP = Rate Of Penetration, m/h
R_{PDC} = PDC radius, mm
TOB = Torque On Bit, daN.m
WOB = Weight On Bit, tons
α = repression angle, degrees
ϕ = rock internal friction angle, degrees
ϕ' = friction angle between crushed rock and virgin rock, degrees
μ = interfacial friction angle between wear flat and rock, degrees
θf = Rock-cutter friction angle, degrees
σ_0 = hydrostatic stress into the crushed zone, Mpa
τ_0 = tangential stress into the crushed zone, MPa
ω_c = Back rake angle, degrees
ω_d = Relief angle, degrees
ω_s = Side rake angle, degrees
ψ = chip failure angle, degrees
ζ = drilling strength, MPa

References

1. Clayton R., Chen S., Lefort G., "New Bit Design, Cutter Technology Extend PDC Applications to Hard Rock Drilling", paper SPE/IADC 91840 presented at the 2005 SPE/IADC Drilling Conference, Amsterdam, Feb. 23-25
2. Gerbaud L., Sellami H., Lamine E., Sagot A., "New PDC Bit Designed Increased Penetration Rate in Slim Wells", paper
3. Mensa-Wilmot G., Penrose B., "Advanced Cutting Structure Improves PDC Bit Performance in Hard and Abrasive Environments", paper SPE 81167 presented at the 2003 Latin American and Caribbean Petroleum Engineer Conference, Trinitad, April 27-30
4. Warren T.M., Brett J.F., Sinor L.A., " Development of a Whirl Resistant Bit", *SPE Drilling Engineering*, 5 (1990) 267-274.
5. Weaver G.E., Clayton R.I., "A New PDC Cutting Structure Improves Bit Stabilization and Extends Application into Harder Rock Types", paper SPE/IADC 25734 presented at the 1993 SPE/IADC Drilling Conference, Amsterdam, Feb 22-25
6. Watson G.R., Barton N.A., Hargrave G.K., "Using New Computational Fluid Dynamics Techniques to Improve PDC Bit Performance", paper SPE/IADC 37580 presented at the 1997 SPE/IADC Drilling Conference, Amsterdam, March 4-6.
7. Menand S., Sellami H., Simon C., Besson A., Da Silva N., "How Bit Profile and Gages Affect the Well Trajectory", paper SPE 74459 presented at the 2002 IADC Drilling Conference, Dallas, Texas, Feb 26-28
8. Finger J.T., Mansure A.J., Knudsen S.D., Jacobson R.D., "Development of a System for Diagnostic-While-Drilling (DWD)", paper SPE/IADC 79884 presented at the 2003 SPE/IADC Drilling Conference, Amsterdam, Feb 19-21
9. Dupriest F.E., Koederitz W.L., "Maximizing Drill Rates with Real-Time Surveillance of Mechanical Specific Energy", paper SPE/IADC 92194 presented at the 2005 SPE/IADC Drilling Conference, Amsterdam, Feb 23-25
10. Sellami H., Fairhurst C., Deliac E., Delbast B., "The role of in situ rock stresses and mud pressure on the penetration rate of PDC Bits", presented at the 1989 International Symposium Rock at Great Depth, Pau, France, Vol. 2, pp. 769-777
11. Detournay E., Defourny P., "A phenomenological model for the drilling action drag bits" International Journal of Rock Mechanism Mining Science, 1992, pp 13-23.
12. Glowka D.A., "Use of Single Cutter Data in the Analysis of PDC Bit Designs: Part 1 – Development of a PDC cutting Force Model", *SPE Journal of Petroleum Technology*, 41 (1989), 797-849.
13. Coudyzer C., Richard T., "Influence of the back and side rake angles in rock cutting", paper AADE-05-NTCE-75 presented at the 2005 AADE Technical Conference and Exhibition, Houston, April 5-7
14. Menand S., " Analyse et validation d'un modèle de comportement directionnel des outils de forage monobloc petit diamètre", *Phd thesis at Ecole des Mines de Paris*, 2001.
15. Kerisel J., "Cours de Mécanique des Sols", Ecole National des Ponts et Chaussées, Paris, p 272
16. Sellami H., "Simulation du travail d'un pic; modélisation de la phase de pénétration", *DEA Ecole des Mines de Paris*, 1984.
17. Challamel N., Sellami H., "Application of yeld Design for Understanding Rock Cutting Mechanism", paper presented at the 1998 SPE/IRSM Eurock 98 conference, Trondheim, July 8-10.
18. Gerbaud L., "Optimisation de l'interaction PDC-Roche : application à la conception d'outils pour forage pétrolier en petit diamètre", *Phd thesis at the Ecole des Mines de Paris*, 1999.
19. Menand S., Sellami H., Simon C., "Classification of PDC bits According to their Steerability", paper SPE/IADC presented at the 2003 Drilling Conference, Amsterdam, The Netherlands, Feb 19-21.
20. Boualleg R., Sellami H., Menand S., Simon C., "Effect of Formations Anisotropy on Directional Tendencies of Drilling Systems", paper SPE/IADC 98865 presented at the 2006 Drilling Conference, Miami, Floride, Feb 21-23.

Metric Convertion Factors

ft x 0.3048 = m
in. x 25.4 = mm
lbf x 4.448 222 = N
ft.lbf x 0.1355818 = daNm

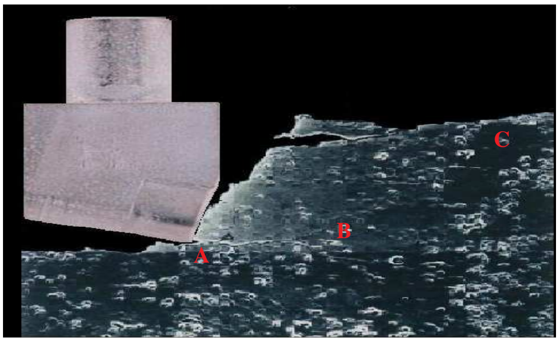

Figure 1 : View of chip formation

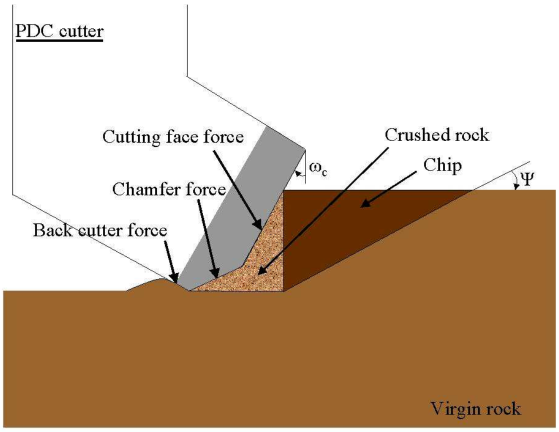

Figure 2 : Idealization of forces acting upon PDC cutter

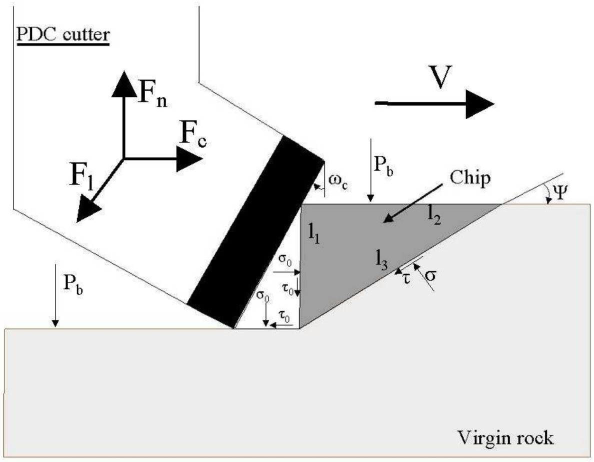

Figure 3 : build up edge of crushed material model

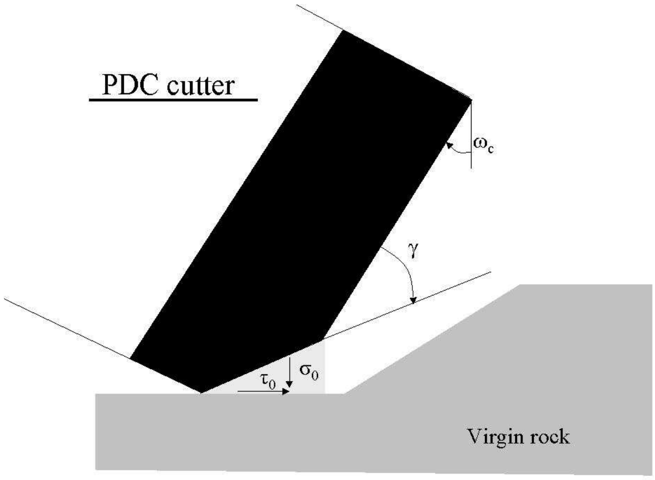

Figure 4 : Stress distribution within the chamfer zone

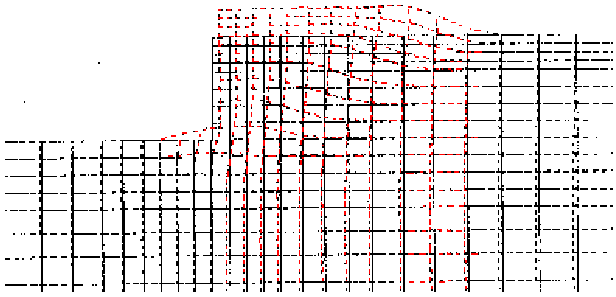

Figure 5 : rock deformation simulation under load with a PDC

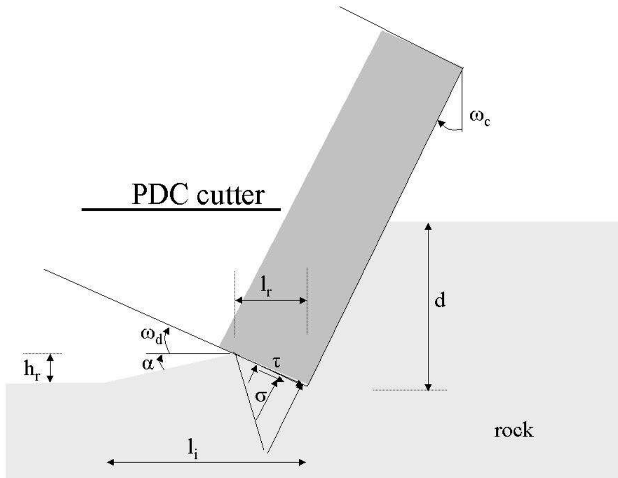

Figure 6 : stress distribution upon the back cutter face

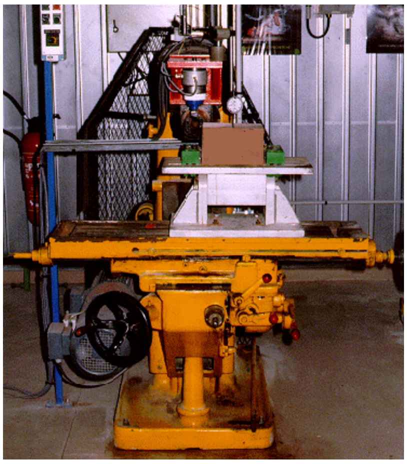

Figure 7 : atmospheric single cutter test stand

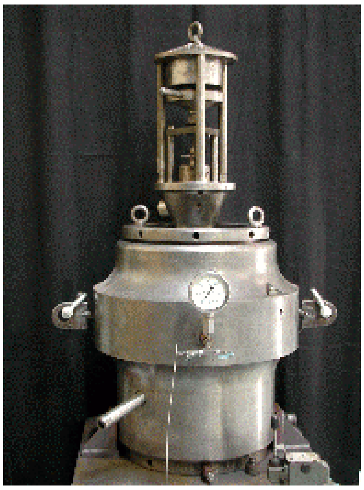

Figure 8 : confinement single cutter test stand

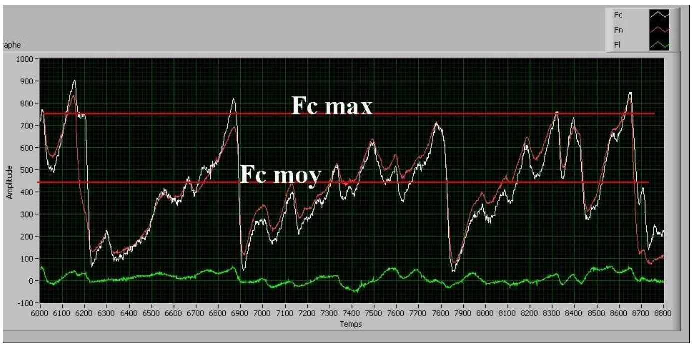

Figure 9 : Experimental PDC forces during rock cutting

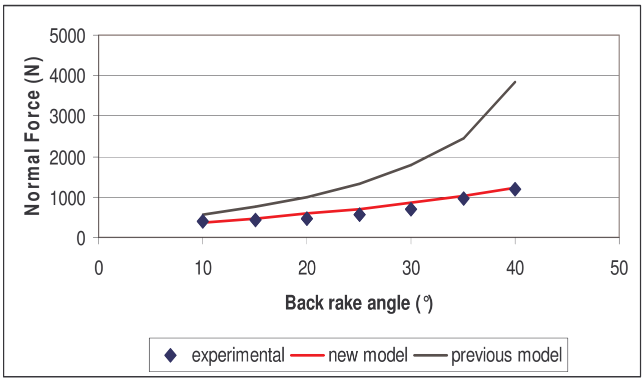

Figure 10 : PDC maximum normal force versus back rake angle

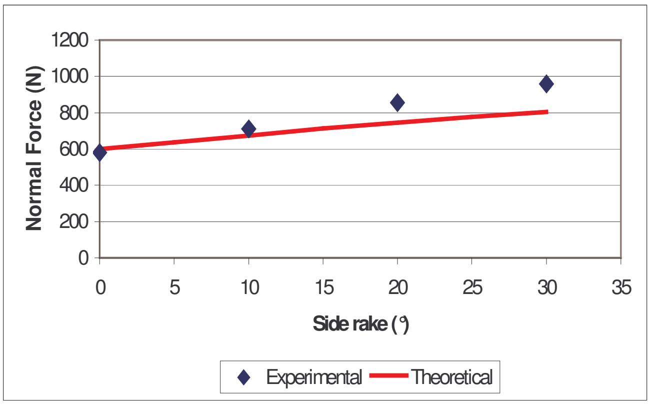

Figure 11 : PDC normal force versus side rack angle for asymetric cut

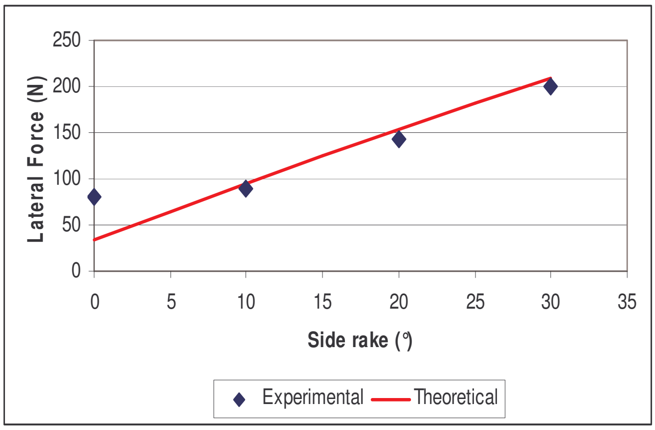

Figure 12 : PDC lateral force versus side rake angle for assymetric cut

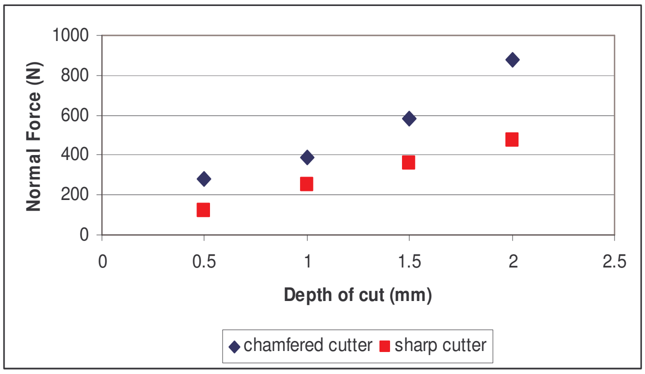

Figure 13 : Normal force on PDC versus depth of cut for sharp and chamfered cutter

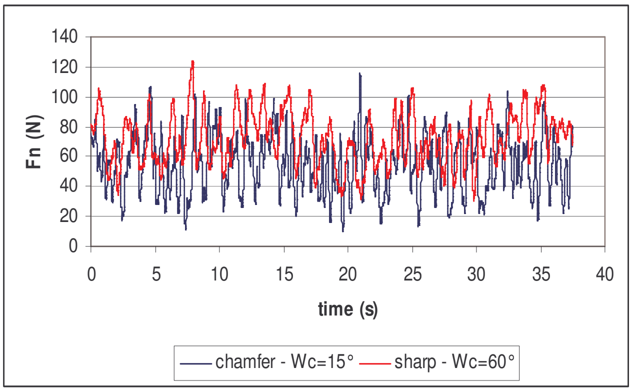

Figure 14 : Normal force evolution for sharp and chamfered cutter at depth of cut equal to 0.15 mm

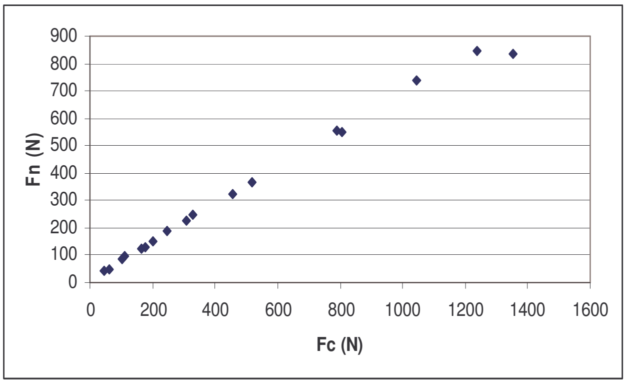

Figure 15 : Evolution of the normal force versus the horizontal force for a sharp cutter

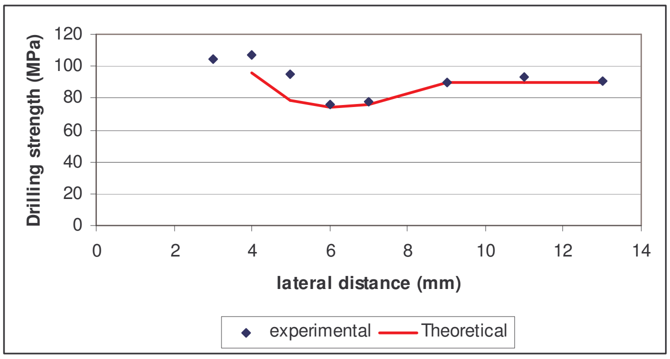

Figure 16 : drilling strength versus lateral distance to pre-existing cut for chamfered PDC

Figure 17 : Full Scale Drilling Test stand

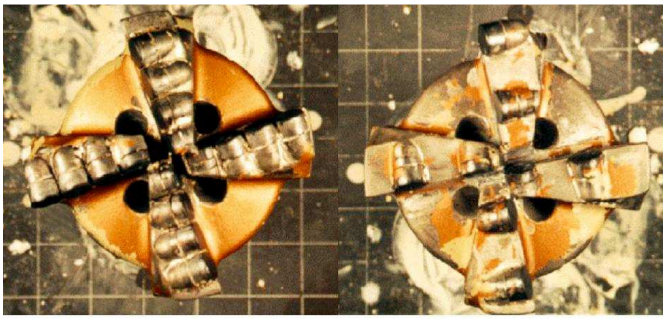

High Density Bit   Low Density Bit

Figure 18 : Special bits designed for understanding PDC bits performances

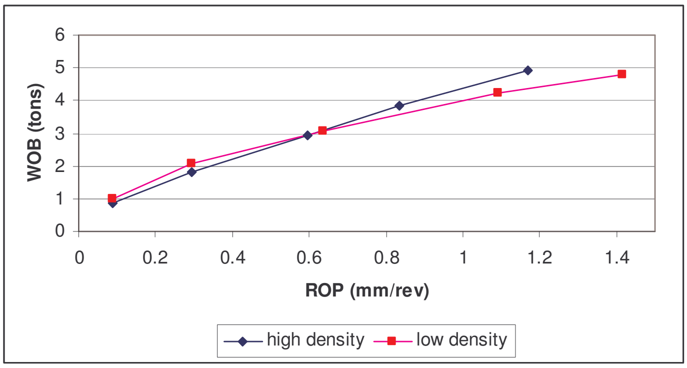

Figure 19 : WOB versus ROP for low and high density bits